

## RESEARCH ARTICLE

# Agarose-based hydrogels with tunable, charge-selective permeability properties

Jing Zhao<sup>1,2,3</sup>  | Matthias Marczynski<sup>1,2</sup>  | Manuel Henkel<sup>1,2</sup>  |  
Oliver Lieleg<sup>1,2</sup> 

<sup>1</sup>TUM School of Engineering and Design, Department of Materials Engineering, Technical University of Munich, Garching, Germany

<sup>2</sup>Center for Protein Assemblies (CPA) and Munich Institute of Biomedical Engineering, Technical University of Munich, Garching, Germany

<sup>3</sup>School of Pharmacy, Shenyang Pharmaceutical University, Shenyang, China

## Correspondence

Oliver Lieleg, TUM School of Engineering and Design, Department of Materials Engineering, Technical University of Munich, Ernst-Otto-Fischer Str. 8, Garching 85748, Germany.  
Email: [oliver.lieleg@tum.de](mailto:oliver.lieleg@tum.de)

## Funding information

Federal Ministry of Education and Research; Free State of Bavaria; Liaoning Provincial Higher Education Overseas Training Program, Grant/Award Number: 2019GJWZD005

## Abstract

Physiologically, a hallmark of biological hydrogels is their ability to selectively trap diffusing molecules and particles. And indeed, there is now increasing interest in using selective hydrogel barriers for applications in biomedicine and medical engineering. However, when employing synthetic polymers to create hydrogels with selective permeabilities, controlling the type and strength of the ensuing filtration process is difficult. Here, we generate hybrid gels with adjustable selectivity profiles by mixing a series of (bio-)macromolecules with agarose. Depending on the type and concentration of the incorporated macromolecules, those hybrid gels achieve a selective retardation of the diffusive translocation of either positively or negatively charged dextrans at both, acidic and neutral pH. Furthermore, we demonstrate three strategies that provide hydrogels with sequestered patches of both, cationic and anionic binding sites, thus creating symmetric charge (i.e., electrostatic bandpass) filters which still allow neutral molecules to pass. Moreover, such agarose matrices offer a high level of versatility as their permeability profiles can be tailored at will by integrating macromolecules with desired physico-chemical properties. Thus, those agarose-based hybrid gels may serve as a powerful platform to engineer adjustable and versatile materials for a broad range of future applications in the field of biomedical engineering.

## KEYWORDS

biopolymers, diffusion barrier, electrostatic interactions, selective filtering

## 1 | INTRODUCTION

Biological hydrogels are strongly hydrated, three-dimensional networks of crosslinked/entangled biopolymers. Depending on their location in the body, they fulfill different functions. However, a common feature that most of those hydrogels share is their ability to trap

certain particles and molecules thereby establishing selective diffusion barriers.<sup>1,2</sup> In addition to playing a pivotal role for physiological processes, hydrogels with selective filtering abilities also have wide applications in industrial or biomedical areas that involve molecular transport processes: examples include drug delivery, tissue engineering, molecular detection, and waste

This is an open access article under the terms of the [Creative Commons Attribution-NonCommercial](https://creativecommons.org/licenses/by-nc/4.0/) License, which permits use, distribution and reproduction in any medium, provided the original work is properly cited and is not used for commercial purposes.

© 2023 The Authors. *Journal of Applied Polymer Science* published by Wiley Periodicals LLC.

removal.<sup>3–7</sup> In all those scenarios, diffusing objects can be filtered by a combination of size exclusion and binding effects.<sup>8</sup> Of course, for smaller objects, that is, nanoparticles and (macro)molecules, binding interactions are typically more efficient in selectively immobilizing them in biological (or artificial) matrices than trapping them according to size; and indeed, there are first examples where biopolymers have been used to develop artificial, charge-selective sieves that can filter out nanoparticles or molecules.<sup>9,10</sup>

There are also synthetic hydrogels with charge-selective permeabilities, and those are usually generated from charged polymers that then bind oppositely charged molecules. For instance, nano-porous hydrogels comprising anionic poly-2-acrylamido-2-methyl-1-propanesulfonic acid can serve as cation-selective filters for the preconcentration of biological samples.<sup>11</sup> Another example are microgels prepared by the polymerization of either cationic acrylamide or anionic acrylic acid, and those gels can be used as sensors for the analysis of charged molecules such as insecticides, drugs, or biomarkers.<sup>12</sup> However, these synthetic hydrogel systems often lack flexibility; adjusting their charge-based trapping properties as well as the strength of the ensuing filtration process is not trivial – but those aspects become important when trying to find a tailored solution that meets the requirements of a specific application. Here, biopolymer-based hydrogel filters may offer more versatility and tunability; yet, many biopolymer-based hydrogel systems suffer from insufficient mechanical stability, and some biopolymers do not even form hydrogels on their own<sup>13,14</sup>—and this limits their use.

Agarose, on the other hand, is an electrostatically neutral polysaccharide that—owing to its ability to form hydrogels with tunable mechanical properties—is already widely used in biomedicine and bioengineering.<sup>15</sup> In fact, this biopolymer can form stable gels even when other biopolymers are incorporated into the matrix.<sup>16</sup> In this context, low gelling-point agarose is particularly interesting as it allows for mixing in heat-sensitive biopolymers at relative low temperature.<sup>16,17</sup> Owing to those properties, agarose might serve as a suitable matrix framework to generate stable hybrid gels with tunable selectivity profiles by mixing in different biopolymers as modulating agents.

Here, we prepare such agarose-based hybrid gels by combining low gelling-point agarose with a series of (bio)macromolecules including the cationic polymers chitosan, polyethylenimine, poly-L-lysine, as well as the anionic molecules mucin, alginate, and  $\gamma$ -polyglutamate. We demonstrate that, with this mixing strategy, stable viscoelastic gels are obtained where the type and concentration of the incorporated (bio)macromolecules

determine the selective barrier properties of the created hybrid material: We can engineer hydrogels that selectively retard the diffusive translocation of either positively or negatively charged dextrans at both, acid and neutral pH. Furthermore, we can modulate the strength of this selective retardation effect by varying the amount of incorporated (bio-)macromolecules. Finally, we demonstrate three strategies of how to obtain hydrogels containing patches of both, cationic and anionic binding sites, that suppress the diffusive translocation of both anionic and cationic dextrans simultaneously while still allowing neutral molecules to pass. Such agarose-based hybrid gels may offer a flexible and sustainable option for numerous applications where the diffusive passage of molecules needs to be precisely regulated.

## 2 | MATERIALS AND METHODS

### 2.1 | Chemicals

Unless stated otherwise, all chemicals used in this study were purchased from Carl Roth GmbH & Co. KG (Karlsruhe, Germany).

### 2.2 | Mucin purification

Porcine gastric mucins were isolated from gastric mucus (which was harvested from pig stomachs) as described in Marczyński et al.<sup>18</sup> In brief, raw mucus was obtained by manual scraping of the inner surface of the gastric tissue with spoons. Then, the collected mucus was diluted 5-fold in 10 mM sodium phosphate buffered saline (PBS; supplemented with 170 mM NaCl sodium chloride and 0.04% [w/v] sodium azide; pH 7.0) and solubilized by stirring at 4°C overnight. Next, the homogenized mucus was subjected to a filtration procedure comprising four subsequent filtering steps through metal grids; here, with each filtering step, the pore size of the mesh decreased (1 mm, 500  $\mu$ m, 200  $\mu$ m, and 125  $\mu$ m). Afterwards, the mucins were isolated by size exclusion chromatography (SEC) using an ÄKTA purifier system (GE Healthcare, Munich, Germany) equipped with an XK50/100 column packed with Sepharose 6FF. The obtained mucin fractions were pooled, and the NaCl concentration in the pooled solution was increased to 1 M. Then, the mucin solution was dialyzed against ultrapure water and concentrated by cross-flow filtration (QuixStand benchtop crossflow system, GE Healthcare) equipped with a hollow fiber module with a molecular weight cut-off of 100 kDa (Xampler Ultrafiltration Cartridge, GE Healthcare). Finally, the concentrate was lyophilized and stored at  $-80^{\circ}\text{C}$  until

TABLE 1 Chemical structure, molecular weight, and zeta potential of the macromolecules used in this study.

Macromolecule	Vendor	Repeating subunit(s)	Molecular weight (kDa)	Zeta potential @pH 4.0 (mV)	Zeta potential @pH 7.0 (mV)
Alginate	Sigma-Aldrich	Mannuronic acid & Guluronic acid	~12–40	−37.1 ± 0.4	−39.3 ± 1.2
γ-Polyglutamate	Sigma-Aldrich	Glutamic acid	~750	−30.0 ± 0.5	−38.4 ± 1.9
Mucin	—	No repeating unit	~3000	−23.1 ± 0.5	−23.2 ± 0.4
Chitosan	HEPPE Medical Chitosan GmbH (Halle, Germany)	D-glucosamine & N-acetyl-D-glucosamine	~25 <sup>a</sup>	36.7 ± 1.2	14.7 ± 1.1
Poly-L-lysine	Sigma-Aldrich	L-Lysine	~30	33.4 ± 2.3	30.1 ± 2.2
Polyethylenimine	Sigma-Aldrich	Ethylenediamine	~0.6–0.8	4.6 ± 3.1	6.3 ± 3.3
Mucin-K <sub>15</sub> C	—	No repeating unit	~3000	−4.7 ± 0.1	−11.5 ± 0.2

<sup>a</sup>As calculated following the Mark-Houwink-Sakurada equation =  $K * M^a$ , with  $K = 1.57$  and  $a = 0.79$ .<sup>20</sup>

further use. We showed previously that these lab-purified mucins are structurally intact and have a better purity than their commercially available analogues. Yet, also carefully purified mucin preparations still contain small amounts of other proteins.<sup>18,19</sup>

### 2.3 | Peptide conjugation to mucins

Lab-purified mucin was functionalized with an oligo-peptide that consists of 15 lysines and one terminal cysteine (K<sub>15</sub>C; PEPperPRINT, Heidelberg, Germany). For this purpose, to reduce disulphide bridges and create free thiol groups, 100 mg of lab-purified mucin were dissolved in 50 mL 20 mM 4-(2-hydroxyethyl)-1-piperazineethanesulfonic acid (HEPES) buffer (pH 7.0; enriched with 10 mM dithiothreitol; DTT) at 4°C for 2 h. Afterwards, the mucin solution was dialyzed (Spectra/Por™ 50 kDa, Spectrum Chemicals Mfg. Corp., New Brunswick, NJ) against ultrapure water at 4°C for 2 days, and the water was exchanged twice during this time. Then, NaCl was dissolved in the mucin solution to a concentration of 1 M. To this solution, 1 mg of the synthetic peptide dissolved in 20 mM HEPES (pH 7.0) were added. Moreover, the oxidizing agent H<sub>2</sub>O<sub>2</sub> was added to a final concentration of 0.1% (v/v). This mixture was allowed to react at room temperature for 2 h. Then, this solution was dialyzed against a 1 M NaCl solution for 1 day at 4°C, followed by dialysis against ultrapure water at 4°C for 2 days. Finally, the solution containing the final mucin-peptide conjugate (mucin-K<sub>15</sub>C) was deep frozen at −80°C and lyophilized.

### 2.4 | Hydrogel preparation

For all macromolecule-enriched hydrogels studied here, an agarose matrix served as a base scaffold. For this

purpose, solid agarose powder (with an ultralow gelling temperature gel point of ≤20°C and low electroendosmosis; Sigma-Aldrich, St. Louis, MO) was dissolved at a concentration of 4% (w/v) in either 10 mM sodium acetate buffer (pH 4.0) or 20 mM HEPES buffer (pH 7.0) during shaking at 70°C, and then cooled to 40°C.

To obtain hydrogels with charge-selective barrier properties, different macromolecules were embedded into the agarose scaffold. All the (bio-)polymers used in this study were previously shown to be stable at the experimental conditions used here—an overview is given in the Supporting Information (Table S1). In detail, a selection of six different macromolecules with net cationic/anionic zeta potentials at both, pH 4.0 and pH 7.0, were employed (see Table 1). The zeta potential values depicted in this table were determined via electrophoretic light scattering using a Litesizer 500 (Anton Paar, Graz, Austria) equipped with a 35 mW laser diode ( $\lambda = 658$  nm). Here, diluted solutions (0.1 mg mL<sup>−1</sup>) of the different macromolecules were analyzed, and 900 μL of each solution were injected into a capillary cuvette (Omega cuvette, Anton Paar) and inserted into the device. Then, the zeta potential was determined in automatic mode ( $T = 25^\circ\text{C}$ , equilibration time: 1 min) using the Smoluchowski approximation of the Henry equation (Henry factor: 1.5).

To obtain functionalized agarose matrices, two-fold concentrated solutions of all macromolecules were prepared in the two buffers. Then, acidic agarose solutions were combined with the acidic macromolecule solutions in a volume ratio of 1:1 and vigorously mixed at 40°C. The same procedure was chosen to prepare the different agarose/macromolecule blends at neutral pH. For all experiments, the same final agarose concentration of 2% (w/v) was used. Once solidified, these agarose-based hybrid gels are structurally stable (Figure S1) and exhibit gel strengths on the order of ~10<sup>3</sup> Pa.

## 2.5 | Rheological characterization

All rheological measurements were conducted on a commercial shear-rheometer (MCR302, Anton Paar, Graz, Austria) equipped with a planar bottom plate (P-PTD200/56, Anton Paar) and a planar measuring head (PP25, Anton Paar). The plate separation was set to 300  $\mu\text{m}$ , and a sample volume of 200  $\mu\text{L}$  was applied. For all samples containing agarose, the system temperature was initially set to 80°C and the agarose (or the agarose/mucin mix) was added in its sol state. Then, to allow for agarose gelation in situ, the measuring head was lowered and the temperature was reduced to 6°C. After a gelation time of 1 min, the viscoelastic material response was quantified. Therefore, the storage modulus  $G'$  and the loss modulus  $G''$  were determined over a frequency range of 0.01–10 Hz. Measurements were conducted in strain-controlled mode using small strain amplitudes corresponding to torques of  $\sim 1 \mu\text{Nm}$ .

## 2.6 | Molecular probes for translocation tests

Owing to both, their well-defined properties and availability with different chemical functionalizations, dextrans were used as test molecules for molecular translocation experiments. In detail, we employed fluorescein isothiocyanate (FITC)-labeled dextran variants with average molecular weights of 4 kDa. (Sigma-Aldrich). We used three such fluorescent dextran variants that differed in their charge properties: unmodified (i.e., electrostatically almost neutral), carboxymethyl-modified (CM, anionic), and diethylaminoethyl-modified (DEAE, cationic) dextrans.

To quantify the charge state of these different dextran variants, the zeta potentials of all three dextran variants dissolved at a concentration of 0.1% (w/v) in either 10 mM acetate buffer (pH 4.0) or 20 mM HEPES buffer (pH 7.0) were determined. These measurements were conducted on a Litesizer 500 (Anton Paar) at a temperature of 25°C using Omega cuvettes (Anton Paar).

## 2.7 | Translocation assay

To study the selective barrier properties of different hydrogels, an assay was developed that allows for quantifying the molecular translocation efficiency across such hydrogel barriers. Here, the hydrogels were reconstituted on top of semi-permeable polycarbonate (PC) membranes (average pore size  $\sim 0.4 \mu\text{m}$ ; Nucleopore Track-Etch Membranes, Whatman plc, Little Chalfont, United Kingdom),

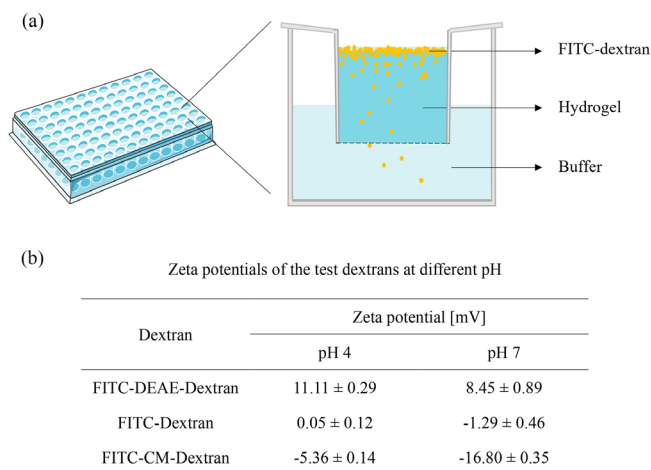


**FIGURE 1** Experimental setup used to investigate the barrier properties of the differently functionalized agarose matrices. (a) Schematic illustration of the 96-well cell culture inserts used for molecular translocation tests across hydrogel barriers. Cell culture inserts which were filled with a hydrogel and then were placed into the wells of 96-well cell culture plates that contained buffer (pH 4 or pH 7). Then, fluorescent dextrans were added on the top of the hydrogel, and the fraction of dextrans that translocated across the hydrogel into the buffer of the acceptor well was determined. (b) Average zeta potential values (together with the standard deviation as obtained from three independent measurements) of the three FITC-Dextran variants used in this study. [Color figure can be viewed at [wileyonlinelibrary.com](http://wileyonlinelibrary.com)]

which were inserted into 96-well cell culture inserts (CellCrown™ inserts; Sigma-Aldrich). These membranes are supposed to allow for the passage of small molecules, whereas the macromolecules comprising the hydrogel should be retained (see Figure 1a for a schematic representation of this assay). For these experiments, the formation of a structurally intact hydrogel on top of the membranes is a vital requirement. To achieve this, the agarose/macromolecule mixtures were directly pipetted on top of the membranes when they were still in a sol state (i.e., the temperature of the mixtures was still above the gelling temperature of agarose, which, according to the vendor, is  $\sim 20^\circ\text{C}$ ). In detail, we added 20  $\mu\text{L}$  of the warm agarose/macromolecule mixture into each cell culture insert; then, the samples were allowed to form gels in situ by keeping them at room temperature for 30 min. After gel formation, the inserts were transferred into the wells of a 96-well microtiter plate (Wuxi NEST Biotechnology Co., Ltd., Wuxi, China), which had been filled with 80  $\mu\text{L}$  of either 10 mM acetate buffer (pH 4.0) or 20 mM HEPES buffer (pH 7.0). Then, a 2  $\mu\text{L}$  drop of the respective buffer containing 5% (w/v) of a certain fluorescently labeled dextran variant (see above) was carefully pipetted on top of the hydrogel, and special care was taken that the gel matrix was not mechanically disturbed. After an incubation step

at room temperature for 6 h, the relative amount of translocated dextran molecules in the acceptor reservoir was determined photometrically at a wavelength of 490 nm (SpectraMax ABS Plus, Molecular Devices, San Jose, CA). This incubation time of 6 h was chosen to be sufficiently larger than the time required for spherical objects with sizes of 2.8 nm (which is the estimated hydrodynamic diameter of the fluorescently labeled 4 kDa dextrans used in this study as provided by the manufacturer) to diffuse unrestrictedly across a distance equal to the thickness of the hydrogel layer used here. The entire procedure of the translocation assay is visualized in a series of photographs shown in Figure S1 (there, for illustrative purposes, blue colored water was employed instead of a FITC-dextran solution). Using the Einstein-Smoluchowski equation and the diffusion equation, and by assuming the local viscosity in the water-based gels to be  $\sim 1$  mPas, we estimated this time to be approximately 2 h and 15 min.

## 2.8 | Stability of the hybrid hydrogels

To assess the stability of hybrid gels, 200  $\mu\text{L}$  of each macromolecule-supplemented agarose hydrogel were prepared as described above and transferred into reaction tubes. Then, 800  $\mu\text{L}$  of a buffer solution (either pH 4.0 or pH 7.0) were added on top of each hybrid gel, and the samples were incubated at 25°C. After 1, 3, 7, and 14 days, the fraction of embedded macromolecules that was released from the agarose matrix into the buffer solution was determined via UV-VIS spectrophotometry (SpectraMax ABS Plus, Molecular Devices). Absorbance spectra and calibration curves obtained for the different macromolecules are shown in the supplement.

## 2.9 | Statistics

All the data shown represents mean values together with the standard deviation; three independent measurements were conducted per condition. To determine significant differences between two examined groups, two-sample t-tests were conducted using a  $p$ -value of  $p = 0.05$ .

# 3 | RESULTS AND DISCUSSION

## 3.1 | Hydrogels with selective permeability properties towards charged dextrans

With the translocation assay employed here, the barrier properties of different (both, biological and synthetic)

hydrogel variants can be quantified by measuring the fraction of different molecular probes that can penetrate the hydrogel in question within a certain time window. Even though this method makes use of macroscopic hydrogel samples, the required amount of hydrogel per well is rather low (20  $\mu\text{L}$  only), and multiple translocation studies can be performed simultaneously in the same 96-well plate format. As molecular probes for these translocation tests, FITC-labeled dextran variants are selected. Those synthetic probe molecules are available in similar molecular weights but with different chemical functionalizations—and the latter allows for comparing dextran variants, which only differ in terms of their net charge (but not in their molecular weights). This is reflected in the zeta potential measurements compiled in Figure 1b: At both pH levels investigated here (i.e., pH 4 and pH 7), the FITC-DEAE-dextrans have cationic properties whereas the FITC-CM-dextrans are anionic. In contrast, dextrans that had not been modified (except for the attachment of the fluorescence label FITC) exhibit almost neutral zeta-potentials, which suggests that they should diffuse more easily across charged hydrogel barriers than their cationic or anionic counterparts.

And indeed, when we compare the translocation efficiency of these three dextran variants across 2% (w/v) mucin hydrogels reconstituted at acidic pH, we find the highest concentration of translocated molecules for the neutral dextrans and the lowest concentration for the cationic ones (Figure 2b). This result was expected as, even at acidic pH levels, porcine gastric mucins are strongly anionic glycoproteins that are physiologically produced by cells in the gastric epithelium. Here, mucin gels constitute a thin layer on the surface of the mucosal tissue and establish a protective barrier against dehydration, pathogen penetration, or the gastric fluid.<sup>21</sup> In previous research, it was found that the barrier properties of such reconstituted mucin gels are strongest towards cationic molecules, which fully agrees with the results obtained here.<sup>13</sup>

However, different from acidic pH, those mucins alone do not form a stable gel at neutral pH (Figure 2a), which makes it difficult to work with them in our translocation assay at those conditions. Thus, to obtain a mechanically stable, mucin-based hydrogel with charge-selective permeability properties at neutral pH, a host matrix is needed that keeps the mucins in place while not affecting the diffusive penetration behavior of small molecules itself.

For this purpose, we here select agarose hydrogels. In detail, agarose, an electrostatically neutral polysaccharide, is employed as a matrix framework into which other macromolecules are embedded by simple mixing. The viscoelastic properties of such agarose (hybrid) hydrogels

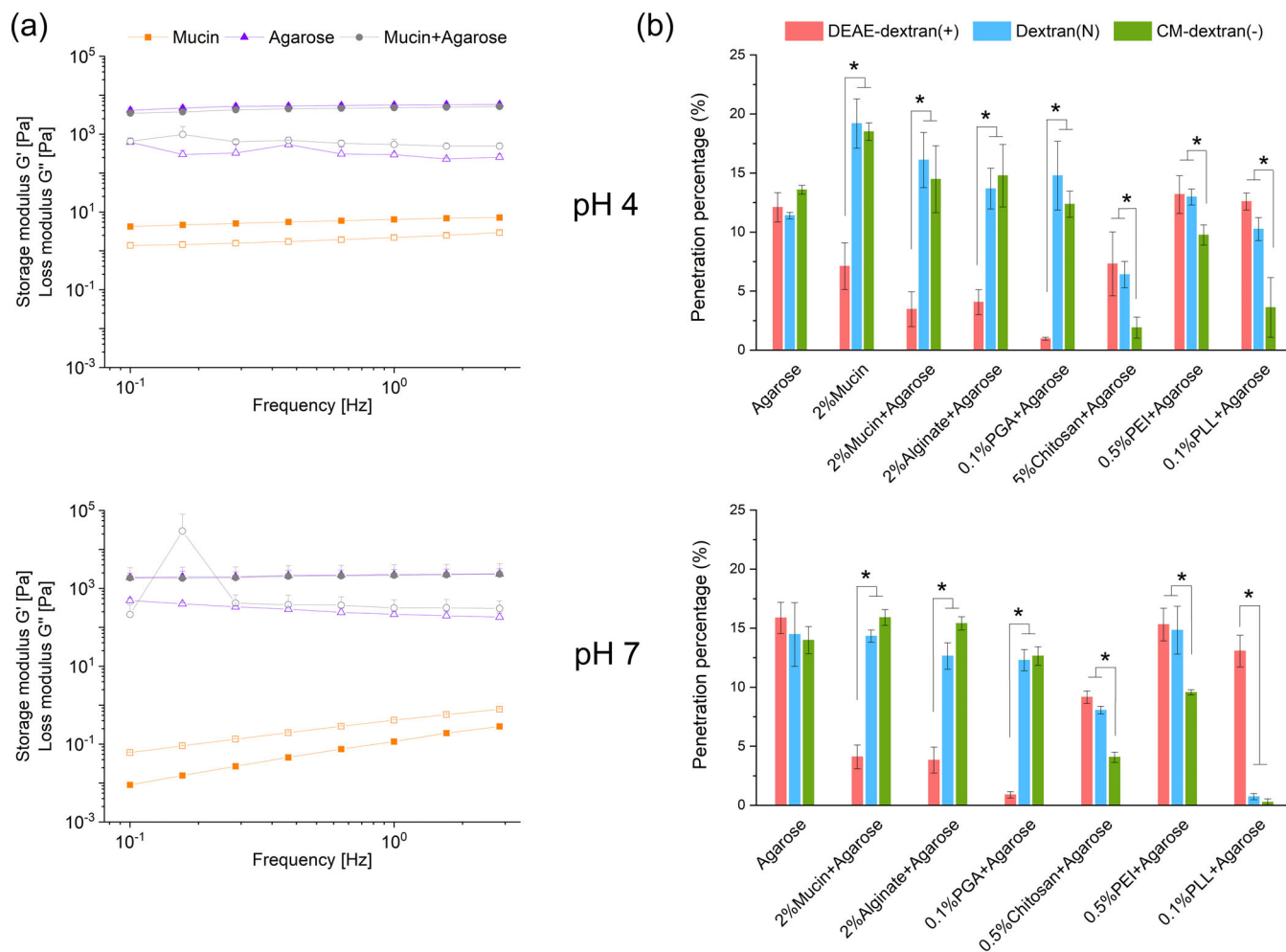


**FIGURE 2** Viscoelastic behavior and permeability properties of agarose-based hydrogels. (a) Viscoelastic moduli of pure mucin, pure agarose, and mixed mucin/agarose systems at pH 4 and pH 7. (b) Penetration percentages of three different dextran variants across different hydrogels reconstituted at pH 4 and pH 7. Error bars denote the standard deviation as determined from three independent measurements. Significant differences (\*) were determined via a two-sample t-test (based on a  $p$ -value of  $p = 0.05$ ). [Color figure can be viewed at [wileyonlinelibrary.com](http://wileyonlinelibrary.com)]

are only dictated by the agarose concentration but are independent of the experimental pH level or the presence of macromolecular additives such as mucin glycoproteins (Figure 2a). In fact, the gelation of agarose hydrogels is based on the formation of hydrogen bonds between agarose molecules, which help stabilizing the helical structure of agarose molecules and their assembly into three-dimensional networks.<sup>22,23</sup> If the macromolecular additives used here were to chemically interact with the agarose network (and thus form additional crosslinks between the agarose fibers), we would expect increased storage moduli compared to a pure agarose gel—yet this is not the case (Figure 2a; gray profiles). Moreover, the permeability properties of a pure agarose hydrogel (2% w/v) do not exhibit any charge-selectivity: As shown in Figure 2b, all three dextran variants can translocate across hydrogels that are composed solely of agarose with

very similar efficiencies—and this holds true at both, pH 4 and pH 7. As this particular agarose variant has a low gelling point, the macromolecule of interest can be added at temperature levels around 40°C, which reduces the risk of heat induced damage to the macromolecular additive.<sup>17</sup>

In a next step, we investigate the barrier properties of agarose hydrogels enriched with 2% (w/v) of mucins. And indeed, for acidic mucin/agarose hybrid gels, we obtain the virtually identical result as for pure mucin gels reconstituted at this pH: also now, the system has charge-selective permeability properties and efficiently retains cationic dextrans while allowing the other two dextran variants to pass (Figure 2b). Control experiments, in which Debye screening was induced (Figure S2), confirm that the selective barrier properties of the mucin/agarose hydrogels are, indeed, brought about by electrostatic

interactions, which allows for partial regeneration of the filtering abilities of such a selective hydrogel (Figure S3). In other words, it is possible to endow an agarose hydrogel with the selective permeability properties of a mucin hydrogel by mixing mucins into it. In addition, with this mixing strategy, we can now generate a stable mucin-based hydrogel matrix at neutral pH (Figure 2a). Also here, we find charge-selective permeability properties, which agrees with the molecular composition of the created hybrid gel.

Having confirmed that integrating anionic mucins into agarose gels allows us to create charge-selective permeability barriers at both, acidic and neutral pH, we next explore the possibility of using other anionic macromolecules instead of mucins to achieve a similar effect. We first test alginate, an anionic polysaccharide that is mainly obtained from brown seaweed. Owing to its biocompatibility, low toxicity and low cost, alginate has been used in various biomedical and bioengineering applications.<sup>24</sup> And indeed, also for an agarose-based hydrogel containing alginate (2% alginate and 2% agarose, w/v), we observe that this hybrid gel selectively hinders the diffusive translocation of cationic dextrans at both, pH 4 and pH 7 (Figure 2b). Consistently, we obtain very similar results when we replace alginate with poly- $\gamma$ -glutamic acid (PGA; this specific polypeptide is the main component of *Bacillus subtilis natto* biofilms and has been investigated in the context of many medical, agricultural and food applications<sup>25</sup>). Here, PGA was added to agarose gels at a lower concentration than mucin and alginate (i.e., at 0.1% (w/v) only) for two reasons: First, when normalized to the molecular weight, PGA has a higher charge density than the other two anionic macromolecules; thus, a lower molar concentration of PGA is sufficient to achieve a comparable number of charged motifs dispersed in the hydrogel matrix (Table 1); second, this lower concentration better agrees with typical PGA concentrations used in the literature (i.e.,  $\leq 0.7\%$  (w/v)) when PGA was employed as a modifying agent in hydrogels.<sup>26,27</sup> Overall, all three agarose gels containing anionic macromolecules as an additive can selectively retard the diffusive translocation of cationic molecules across the hydrogel barrier.

In a next step, we aim at creating hydrogel barriers that allow cationic molecules to pass reasonably well but, instead, retard the translocation of anionic ones. For this purpose, we select three cationic macromolecules, that is, chitosan,<sup>28</sup> polyethylenimine (PEI),<sup>29,30</sup> and poly-L-lysine (PLL)<sup>31</sup> (and all three compounds have been described to be biocompatible with applications in the biomedical sector such as drug delivery, tissue transplantation, and wound treatment). As expected, at both pH levels, those hybrid gels significantly retard the diffusive translocation of anionic molecules compared to neutral and cationic ones (Figure 2b).

There is one condition, however, that deserves a more detailed discussion: for the PLL/agarose hybrid hydrogel reconstituted at neutral pH, also the “neutral” (= unmodified) dextrans were efficiently restricted. At this point, it is important to realize two facts: first, poly-L-lysine carries a very high density of primary amines, which can be easily protonated and thus endow PLL with a very high positive charge density—even at neutral pH (see Table 1); thus, PLL can be expected to bind anionic molecule more efficiently than the other two cationic macromolecular additives used here.<sup>31,32</sup> Second, according to the zeta potential measurements shown in Figure 1b (which agree with results reported in the literature<sup>33</sup>), the unmodified (‘neutral’) FITC-dextrans are actually weakly anionic at neutral pH—and this weak anionic character is brought about by the fluorophore FITC. Taken together, those two items can explain why PLL/agarose hybrid gels also pose a strong barrier towards those weakly anionic molecules at neutral pH (but not at acidic pH where the “neutral” dextran variant is, in fact, almost charge neutral).

### 3.2 | Hydrogels with tuneable levels of selective permeability

Having shown that we can create hydrogels that selectively retard the diffusive translocation of either cationic or anionic molecules, we next ask if the strength of this effect can be tuned. To achieve this, we vary the concentration of the added macromolecules in the agarose matrix. For those tests, mucin and chitosan are selected as representatives of cationic and anionic additives, respectively (Figure 3); in each case, the concentration of the added macromolecule is varied over an order of magnitude. And indeed, for mucin/agarose hybrid gels, we obtain barriers (at both, acidic and neutral pH) that increasingly suppress the translocation of cationic dextrans as more mucins are integrated into the agarose matrix. Interestingly, whereas the gel permeability towards neutral and anionic dextrans remains virtually unchanged until a mucin content of 2% (w/v), we observe a marked reduction in the translocation efficiency of those two off-target molecules once a mucin concentration of 4% (w/v) is reached. Probably, as mucins are very large macromolecules, this effect is due to a reduced mesh size of this hybrid network that limits the diffusive spreading of all dextrans at this high mucin concentration.<sup>34</sup>

Similarly, for chitosan/agarose hybrid gels containing different amounts of the cationic macromolecule chitosan, barriers with stronger barrier properties towards anionic dextrans are obtained (at both pH levels) as the chitosan concentration is increased from 0.05% (w/v) to

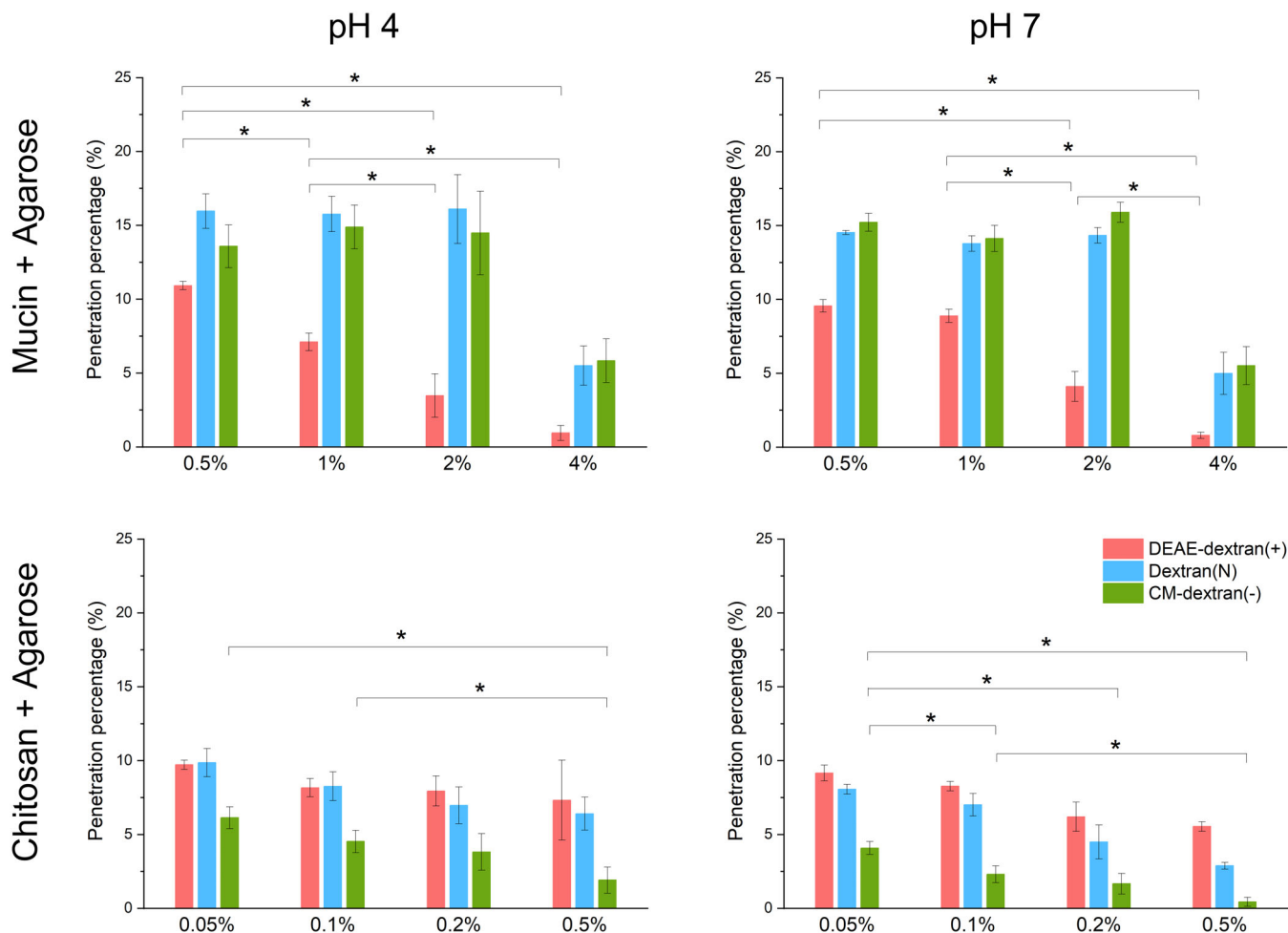


**FIGURE 3** Tuning the permeability properties of selected macromolecule/agarose hybrid gels. In these hybrid gels, the concentration of the selectivity conveying macromolecular component (i.e., either mucin or chitosan) is gradually increased. Error bars denote the standard deviation as determined from three independent measurements. Significant differences (\*) were determined via a two-sample t-test (based on a  $p$ -value of  $p = 0.05$ ). [Color figure can be viewed at [wileyonlinelibrary.com](http://wileyonlinelibrary.com)]

0.5% (w/v); Figure 3. Here, steric hindrance effects limiting the diffusive penetration of the two off-target molecules at higher additive concentrations occur as well but are less pronounced than for mucin/agarose gels. We attribute this to the fact that chitosans are smaller macromolecules than mucins and—owing to differences in solubility—were here added to the agarose host matrix in much lower concentrations than the mucins.

### 3.3 | Hydrogels with electrostatic bandpass permeability

So far, we have prepared different macromolecule/agarose hybrid gels such that they selectively retard the diffusive translocation of either cationic or anionic molecules. In a next step, we ask if we can also suppress the diffusion of both types of charged molecules at the same

time while still allowing the neutral molecules to easily penetrate the hydrogel barrier. To achieve this, we aim at preparing a hydrogel that contains patches of both, positive and negative charges. In such an environment, electrostatic binding interactions should be possible with anionic and cationic molecules—albeit at different locations of the gel matrix.

Our first strategy makes use of mixing two different macromolecules into the agarose matrix, namely polycationic chitosan and polyanionic mucin. And indeed, as shown in Figure 4a, such mucin/chitosan/agarose triplemixtures lead to the desired outcome at both, acidic and neutral pH (with a more symmetric result at pH 4). However, when we macroscopically inspect those triplemixture gels, we detect macromolecule aggregates that are clearly visible to the naked eye throughout the sample. Most likely, those represent complexes of chitosans and mucins whose formation is facilitated by attractive

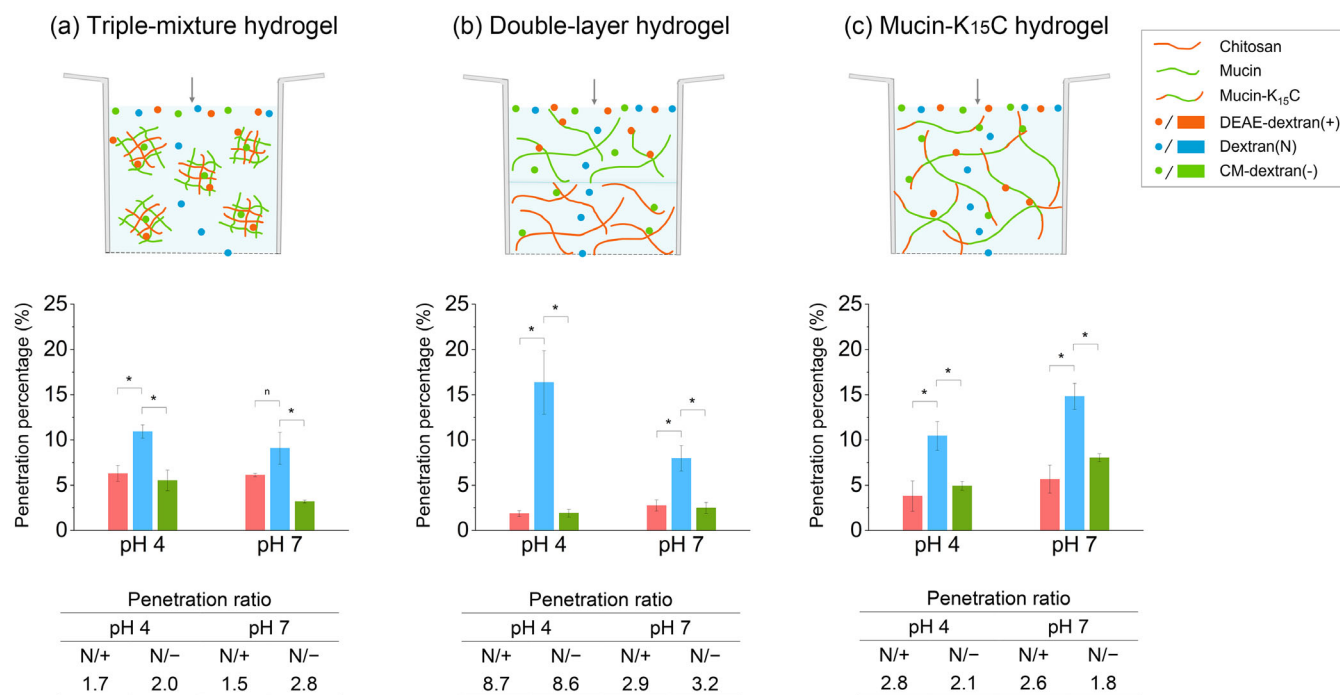


**FIGURE 4** Agarose-based hydrogels with symmetric permeability properties. As illustrated by the schematics shown in the top row, three strategies are shown of how to obtain hydrogels that retard the diffusive penetration of anionic and cationic molecules at the same time: (a) a triple-mixture hydrogel containing 2% mucin, 0.2% chitosan, and 2% agarose; (b) a double-layer hydrogel comprising a bottom layer of 2% mucin/2% agarose and a top layer of 0.2% chitosan/2% agarose; (c) a 2% mucin/2% agarose hybrid hydrogel, where the mucin was covalently functionalized with the cationic peptides K<sub>15</sub>C. The tables below the bar plots depict the penetration ratios of neutral dextrans with respect to their cationic (N/+) and anionic (N/-) counterparts. Error bars denote the standard deviation as determined from three independent measurements. Significant differences (\*) were determined via a two-sample *t*-tests (based on a *p*-value of *p* = 0.05). [Color figure can be viewed at [wileyonlinelibrary.com](http://wileyonlinelibrary.com)]

electrostatic forces acting between the two components (Figure 4a). Such a cluster formation of the selected macromolecular additives has been described in the literature previously.<sup>35,36</sup> We can confirm this observation by performing phase-contrast microscopy of binary mucin/chitosan mixtures in aqueous solutions at both, acidic and neutral pH conditions (Figure S4).

The observed cluster formation may also explain the only moderate retardation effect we observe for the charged dextrans: macromolecule cluster formation will reduce the amount of exposed charged areas on both, the chitosans and mucins; this, in turn, will impede the capturing efficiency of either macromolecule towards charged dextrans.

Therefore, to avoid such aggregate formation, we modify our strategy and create a double-layer gel, which only contains binary macromolecule mixtures in either layer: mucin/agarose in the top layer and chitosan/agarose in the bottom layer. When dextrans are added on top of this double-layer gel, they need to translocate both sublayers, and this should allow the system to sequentially trap both dextran variants: first, the cationic ones in the top layer; then, the anionic ones in the bottom layer.

As expected, this double-layer hydrogel has a more efficient barrier effect on the charged dextrans (Figure 4b) than the triple-mixture discussed above. Especially at acidic pH, the retardation factor (i.e., the ratio of translocated charged dextrans with respect to the uncharged ones) is increased from  $\sim 2$  to a factor of 8–9.

Still, also this double-layer system comes with its limitations: to achieve the desired filtering effect, it requires the diffusing molecules to pass the gel in a certain direction. Moreover, two different hydrogel layers need to be prepared on top of each other, which renders the fabrication of this particular diffusion barrier a bit more complex than the systems discussed so far. Hence, in a third approach, we aim at engineering a hydrogel with similar symmetric filtration abilities based on one macromolecular additive only. For this purpose, we choose a semi-synthetic approach where we modify mucin glycoproteins before we integrate them into the agarose matrix. In detail, we covalently link cationic peptides (K<sub>15</sub>C) to the mucins via disulfide bridges (see Table 1 for pH-dependent charge properties). Such mucin-peptide/agarose hybrid gels have a clear and uniform appearance without any signs of aggregate formation. Moreover,

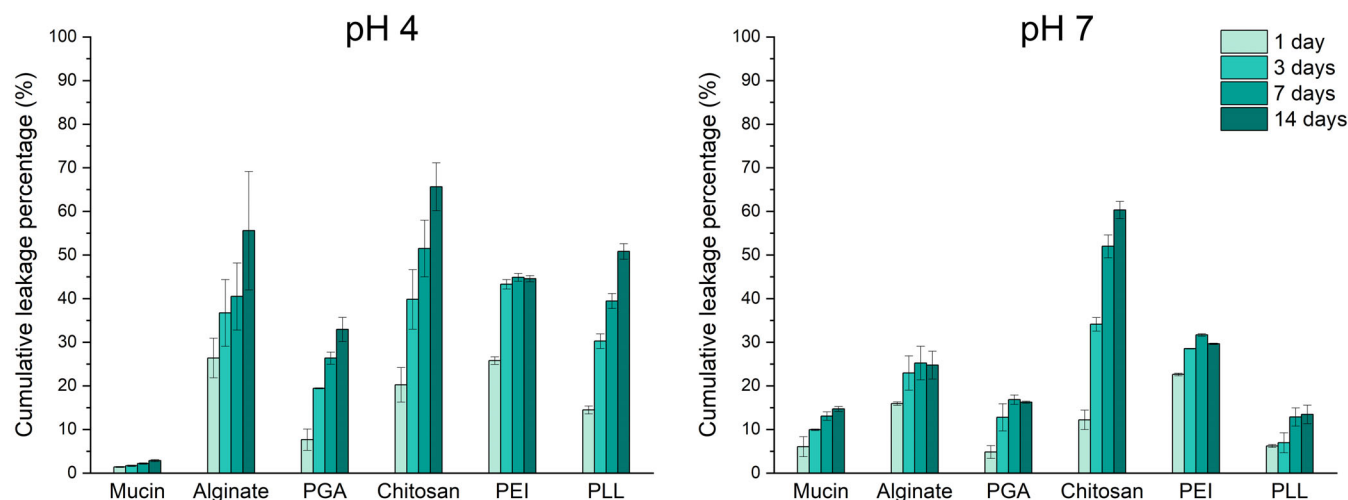


**FIGURE 5** Stability of the hybrid hydrogels. Cumulative leakage percentages of the added polymers from the hybrid hydrogels during a time span of 14 days (storage at room temperature). Error bars denote the standard deviation as determined from three independent measurements. [Color figure can be viewed at [wileyonlinelibrary.com](http://wileyonlinelibrary.com)]

those semi-synthetic macromolecular gels act as diffusive barriers towards both cationic and anionic dextrans but allow the neutral dextrans to pass (Figure 4c)—and this strategy works at both pH levels. In other words, it is very well possible to endow an unselective agarose hydrogel with complex charge-selective barrier properties by depositing both, positive and negative charge patches in the gel matrix.

Interestingly, with our second experimental setup (i.e., the layered hydrogel), we detect a statistically significant impact of the experimental pH on the filtering capacity of the bifunctional gels towards charge-neutral dextrans but not towards anionic or cationic dextrans (Figure 4b). We attribute this effect to the change of the zeta potential of FITC-dextrans from neutral at pH 4.0 to slightly anionic at pH 7.0 (Figure 1b). Accordingly, this negative charge at neutral pH results in an overall retardation of the translocation process due to binding of the dextrans to amines in the chitosan layer. In contrast, the sign of the zeta potential does not change for the other two dextran variants, and thus a change of the experimental pH level from 4.0 to 7.0 does not affect their translocation efficiencies (Figure 4b).

### 3.4 | Assessing the stability of the created hybrid gels

In the hybrid gels presented here, the added (bio-)macromolecules are embedded into the agarose hydrogels by simple physical mixing, and, owing to the rather inert nature of agarose molecules, we attribute their integration into the agarose scaffold mainly to physical

entanglements. To assess how well the different polymers are integrated into the agarose mesh, in a last step, we assess the stability of these hybrid gels over time. This will provide an estimate of how long the different systems will be able to act as a selective filtration matrix. To do so, the leakage behavior of the different (bio-)macromolecular additives from the agarose host matrices is investigated (Figure 5) by incubating the hybrid gels in buffer solutions for up to 2 weeks and determining the fraction of macromolecules released into the buffer phase spectroscopically (see Figures S5, S6, and S7 for absorption spectra and calibration curves).

Among all hybrid gels tests, the mucin/agarose mix shows the best stability—especially at acidic pH. Here, the ability of mucins to form a polymeric network in an acidic environment might explain this result as this effect will certainly help keeping the mucins in place.<sup>37,38</sup> However, also at neutral pH (where the mucins cannot form a network on their own), leakage of mucins is low: even after 2 weeks of incubation in pH-neutral buffer, we find that only ~15% of the initially integrated mucins have left the hybrid gel. Probably, the high molecular weight of mucins and the ensuing high chain length of the macromolecules gives rise to high levels of physical entanglements with each other and—more importantly—with the agarose molecules of the host matrix, and those entanglements will considerably slow down the diffusive leaching of the additive from the host matrix. At neutral pH, we find a similar good stability for PGA/agarose and PLL/agarose gels, and reasonable stability (with leakage percentages of 30% or less) for PEI/agarose gels at neutral pH and PGA/agarose gels at acidic pH. Notably, independent of the experimental pH, PEI molecules seem to leak

from the hydrogel matrix more rapidly than the other polymers, that is, within a rather short time window of 1 day (Figure 5). This may be rationalized by the low molecular weight, and thus comparably small size, of the PEI employed here compared to the other polymers, which may allow for a more rapid disentanglement due to reptation. For the remaining systems (especially for hybrid gels containing chitosan) to be employed as filtration matrices for long-term usage, their stability might need to be improved as the intermolecular hydrogen bonds acting between the additive and the agarose host matrix appear not to be strong enough to prevent leakage.<sup>39</sup> Here, three strategies could be considered: First, stabilizing the agarose host matrix itself (e.g., by adding the naturally occurring cross-linker molecule genipin<sup>40</sup>) might help—especially if a certain application calls for improving the thermal stability of the created hybrid matrix. Second, employing an additional cross-linking step to fix the added (bio-)macromolecules to the host matrix could be a helpful approach—and there are already examples in the literature of how to achieve this for chitosan/agarose gels<sup>41,42</sup> (which are the ones that—in our setup—were most prone to additive leakage over time). Third, one could also cross-link the added biopolymers to each other. This could be achieved by employing methacrylated mucins and exposing them to UV light,<sup>43</sup> by crosslinking PLL with ethylene glycol diglycidyl ether,<sup>44</sup> or by introducing ionic cross-links into alginate, chitosan, PEI, or  $\gamma$ -PGA networks.<sup>45–47</sup> However, it might strongly depend on the particular hydrogel mixture, which of those three strategies turns out to be the most efficient one.

## 4 | CONCLUSIONS

For several applications, for instance in the fields of tissue engineering or molecular sensing, it would be often desirable to achieve control over the diffusive penetration behavior of different objects with differing physicochemical properties. In this study, we achieve such control over the diffusive translocation of molecular probes across agarose gels by embedding different (bio-)macromolecules into the agarose matrix. Specifically, integrating charged (bio-)polymers into an agarose scaffold allowed for tuning the permeability of the hydrogels towards charged (cationic or anionic) molecules. This approach, however, is not limited to engineering an asymmetric charge filter. In fact, through chemically modifying poly-anionic mucins by grafting cationic oligo-lysines to cysteine residues we were able to create polymers with modified charged patterns. Mixing these modified mucins into an agarose matrix allowed us to obtain hydrogels

with bandpass filtering properties (i.e., a hydrogel that selectively filtered out cationic and anionic molecules but allowed uncharged molecules to pass). Of course, such hydrogel-based molecular filtering approaches do not need to be limited to charge-based filtering. In fact, a number of other physical properties or chemical groups could be exploited to create selective hydrogel filters. For instance, a similar approach could be employed to achieve selective filtering based on hydrophobicity or affinity towards certain motifs presented by the polymeric scaffold (such as hexa-histidine tags or biotin residues). Moreover, by making use of macromolecular additives that change their configuration in response to external stimuli (e.g., temperature alterations), hydrogels may be created, which exhibit switchable filtering properties upon exposure to certain cues. Thus, the strategy presented here presents a versatile platform to create a multitude of different hydrogel barriers with adjustable (and maybe even dynamically tuneable) selectivity properties.

## AUTHOR CONTRIBUTIONS

**Jing Zhao:** Data curation (lead); formal analysis (equal); visualization (lead); writing – original draft (lead). **Matthias Marczyński:** Conceptualization (equal); data curation (supporting); formal analysis (equal); writing – original draft (supporting). **Manuel Henkel:** Data curation (supporting). **Oliver Lieleg:** Conceptualization (equal); supervision (lead); writing – review and editing (lead).

## ACKNOWLEDGMENTS

This project was funded by the Federal Ministry of Education and Research (BMBF) and the Free State of Bavaria under the Excellence Strategy of the Federal Government and the Länder through the ONE MUNICH Project Munich Multiscale Biofabrication. We thank Tobias Fuhrmann for assistance with the mucin purification. Jing Zhao acknowledges support by the Liaoning Provincial Higher Education Overseas Training Program (2019GJWZD005) and acknowledges Prof. Dr. Shirui Mao from School of Pharmacy, Shenyang Pharmaceutical University, Shenyang, China for her help with obtaining this funding. Open Access funding enabled and organized by Projekt DEAL.

## CONFLICT OF INTEREST STATEMENT

The authors declare no conflicts of interest.

## DATA AVAILABILITY STATEMENT

The data that support the findings of this study are available from the corresponding author upon reasonable request.

## ORCID

Jing Zhao  <https://orcid.org/0000-0002-5328-3759>

Matthias Marczyński  <https://orcid.org/0000-0001-6681-1891>

Manuel Henkel  <https://orcid.org/0000-0001-5345-6325>

Oliver Lieleg  <https://orcid.org/0000-0002-6874-7456>

## REFERENCES

- [1] O. Lieleg, K. Ribbeck, *Trends Cell Biol.* **2011**, *21*, 543.
- [2] J. Witten, T. Samad, K. Ribbeck, *Curr. Opin. Biotechnol.* **2018**, *52*, 124.
- [3] A. C. Daly, L. Riley, T. Segura, J. A. Burdick, *Nat. Rev. Mater.* **2020**, *5*, 20.
- [4] A. Ali, S. Ahmed, *J. Agric. Food Chem.* **2018**, *66*, 6940.
- [5] X. Liu, J. Liu, S. Lin, X. Zhao, *Mater. Today* **2020**, *36*, 102.
- [6] B. O. Okesola, D. K. Smith, *Chem. Soc. Rev.* **2016**, *45*, 4226.
- [7] M. Steinacher, A. Cont, H. Du, A. Persat, E. Amstad, *ACS Appl. Mater. Interfaces* **2021**, *13*, 15601.
- [8] J. L. Schiller, S. K. Lai, *ACS Appl. Bio. Mater.* **2020**, *3*, 2875.
- [9] T. Chakrabarty, V. K. Shahi, *RSC Adv.* **2014**, *4*, 53245.
- [10] B. Winkeljann, B. T. Käs Dorf, J. Boekhoven, O. Lieleg, *Macromol. Biosci.* **2018**, *18*, 1700311.
- [11] H. Kim, J. Kim, E.-G. Kim, A. J. Heinz, S. Kwon, H. Chun, *Biomicrofluidics* **2010**, *4*, 043014.
- [12] D. J. Kim, S.-G. Park, D.-H. Kim, S.-H. Kim, *Small* **2018**, *14*, 1802520.
- [13] M. Marczyński, B. T. Käs Dorf, B. Altaner, A. Wenzler, U. Gerland, O. Lieleg, *Biomater. Sci.* **2018**, *6*, 3373.
- [14] R. M. Felfel, M. J. Gideon-Adeniyi, K. M. Zakir Hossain, G. A. F. Roberts, D. M. Grant, *Carbohydr. Polym.* **2019**, *204*, 59.
- [15] M. Beaumont, R. Tran, G. Vera, D. Niedrist, A. Rousset, R. Pierre, V. P. Shastri, A. Forget, *Biomacromolecules* **2021**, *22*, 1027.
- [16] M. Khodadadi Yazdi, A. Taghizadeh, M. Taghizadeh, F. J. Stadler, M. Farokhi, F. Mottaghitalab, P. Zarrintaj, J. D. Ramsey, F. Seidi, M. R. Saeb, M. Mozafari, *J. Controlled Release* **2020**, *326*, 523.
- [17] K. Y. Cheung, W. C. Mak, D. Trau, *Anal. Chim. Acta* **2008**, *607*, 204.
- [18] M. Marczyński, C. A. Rickert, T. Fuhrmann, O. Lieleg, *Sep. Purif. Technol.* **2022**, *294*, 121209.
- [19] M. Marczyński, K. Jiang, M. Blakeley, V. Srivastava, F. Vilaplana, T. Crouzier, O. Lieleg, *Biomacromolecules* **2021**, *22*, 1600.
- [20] M. R. Kasaai, J. Arul, G. Charlet, *J. Polym. Sci., Part B: Polym. Phys.* **2000**, *38*, 2591.
- [21] D. Larobina, A. Pommella, A.-M. Philippe, M. Y. Nagazi, L. Cipelletti, *Proc. Nat. Acad. Sci.* **2021**, *118*, e2103995118.
- [22] S. Arnott, A. Fulmer, W. Scott, I. Dea, R. Moorhouse, D. Rees, *J. Mol. Biol.* **1974**, *90*, 269.
- [23] M. Tako, S. Nakamura, *Carbohydr. Res.* **1988**, *180*, 277.
- [24] K. Y. Lee, D. J. Mooney, *Prog. Polym. Sci.* **2012**, *37*, 106.
- [25] L. Wang, S. Chen, B. Yu, *Trends Food Sci. Technol.* **2022**, *119*, 1.
- [26] S. H. Cho, A. Kim, W. Shin, M. B. Heo, H. J. Noh, K. S. Hong, J. H. Cho, Y. T. Lim, *Int. J. Nanomed.* **2017**, *12*, 2607.
- [27] C.-C. Lin, J.-Y. Chiu, *Polymer* **2021**, *230*, 124049.
- [28] N. Morin-Crini, E. Lichtfouse, G. Torri, G. Crini, *Environ. Chem. Lett.* **2019**, *17*, 1667.
- [29] A. P. Pandey, K. K. Sawant, *Mater. Sci. Eng. C* **2016**, *68*, 904.
- [30] C. Wiegand, M. Bauer, U.-C. Hipler, D. Fischer, *Int. J. Pharm.* **2013**, *456*, 165.
- [31] N. A. Patil, B. Kandasubramanian, *Eur. Polym. J.* **2021**, *146*, 110248.
- [32] H. Tian, L. Lin, Z. Jiao, Z. Guo, J. Chen, S. Gao, X. Zhu, X. Chen, *J. Controlled Release* **2013**, *172*, 410.
- [33] E. Schuster, A.-M. Hermansson, C. Öhgren, M. Rudemo, N. Lorén, *Biophys. J.* **2014**, *106*, 253.
- [34] K. T. H. Nguyen, E. V. Mathias, E. Porter, Y. Ba, *J. Incl. Phenom. Macrocycl. Chem.* **2016**, *86*, 273.
- [35] M. P. Deacon, S. McGurk, C. J. Roberts, P. M. Williams, S. J. B. Tendler, M. C. Davies, S. S. Davis, S. E. Harding, *Biochem. J.* **2000**, *348*, 557.
- [36] I. A. Sogias, A. C. Williams, V. V. Khutoryanskiy, *Biomacromolecules* **2008**, *9*, 1837.
- [37] X. Cao, R. Bansil, K. R. Bhaskar, B. S. Turner, J. T. LaMont, N. Niu, N. H. Afdhal, *Biophys. J.* **1999**, *76*, 1250.
- [38] R. Bansil, B. S. Turner, *Curr. Opin. Colloid Interface Sci.* **2006**, *11*, 164.
- [39] V. Zamora-Mora, D. Velasco, R. Hernández, C. Mijangos, E. Kumacheva, *Carbohydr. Polym.* **2014**, *111*, 348.
- [40] R. Meena, K. Prasad, A. K. Siddhanta, *J. Appl. Polym. Sci.* **2007**, *104*, 290.
- [41] L. G. Gómez-Mascaraque, J. A. Méndez, M. Fernández-Gutiérrez, B. Vázquez, J. San Román, *Acta Biomater.* **2014**, *10*, 798.
- [42] M. Bilal, T. Rasheed, Y. Zhao, H. M. N. Iqbal, *Int. J. Biol. Macromol.* **2019**, *124*, 742.
- [43] T. M. Lutz, C. Kimna, O. Lieleg, *Int. J. Biol. Macromol.* **2022**, *215*, 102.
- [44] K. Matsumoto, A. Kawamura, T. Miyata, *Chem. Lett.* **2015**, *44*, 1284.
- [45] Z. Li, Z. Lin, *Aggregate* **2021**, *2*, e21.
- [46] A. Movahedi, A. Lundin, N. Kann, M. Nydén, K. Moth-Poulsen, *Phys. Chem. Chem. Phys.* **2015**, *17*, 18327.
- [47] M. Kretschmer, O. Lieleg, *Biomater. Sci.* **2020**, *8*, 1923.

## SUPPORTING INFORMATION

Additional supporting information can be found online in the Supporting Information section at the end of this article.

**How to cite this article:** J. Zhao, M. Marczyński, M. Henkel, O. Lieleg, *J. Appl. Polym. Sci.* **2023**, *140*(34), e54303. <https://doi.org/10.1002/app.54303>